



# Stabilizing control of two-wheeled wheelchair with movable payload using optimized interval type-2 fuzzy logic

Journal of Low Frequency Noise,  
Vibration and Active Control  
0(0) 1–22  
© The Author(s) 2020  
DOI: 10.1177/1461348420979480  
[journals.sagepub.com/home/lfn](https://journals.sagepub.com/home/lfn)  
 SAGE

Nurul Fadzlina Jamin<sup>1</sup> , Nor Maniha Abdul Ghani<sup>1</sup>,  
Zuwairie Ibrahim<sup>2</sup>, Ahmad Nor Kasruddin Nasir<sup>1</sup>,  
Mamunur Rashid<sup>1</sup> and Mohammad Osman Tokhi<sup>3</sup>

## Abstract

The control schemes of a wheelchair having two wheels with movable payload utilizing the concept of a double-link inverted pendulum have been investigated in this article. The proposed wheelchair has been simulated using SimWise 4D software considering the most efficient parameters. These parameters are extracted using the spiral dynamic algorithm while being controlled with interval type-2 fuzzy logic controller (IT2FLC). The robustness and stability of the implemented controller are assessed under different situations including standing upright, forward motion and application of varying directions and magnitudes of outer disturbances to movable (up and down) system payload. It is shown that the two-wheeled wheelchair adopted by the newly introduced controller has achieved a 94% drop in torque for both Link1 and Link2 and more than 98% fall in distance travelled in comparison with fuzzy logic control type-1 (FLCT1) controller employed in an earlier design. The present study has further considered the increased nonlinearity and complexity of the additional moving payload. From the outcome of this study, it is obvious that the proposed IT2FLC-spiral dynamic algorithm demonstrates better performance than FLCT1 to manage the uncertainties and nonlinearities in case of a movable payload two-wheel wheelchair system.

## Keywords

Two-wheeled wheelchair, stability, fuzzy logic, payloads, spiral dynamic algorithm

## Introduction

Wheelchairs are considered as a critical resource for ensuring mobility for both the elderly and physically impaired people. It is important to assure that the targeted users are able to perform their daily activities securely without the help of others. Moreover, the safety features of a wheelchair are given the highest priority to ensure the comfortability and protection of targeted users. Hence, particular emphasis is given to achieve shorter travel distances and improve stability together with poor torques, taking into account both foreseen and unforeseen disturbances. The basic wheelchair configuration is fundamentally constructed in a conventional four-wheeled style. Although the traditional wheelchair offers mobility, it introduces several drawbacks due to its structure and control mechanism. These drawbacks include the inadequacy of height adjustment that restricts their vertical reach and the bulky nature that creates complications in moving in confined spaces. These issues can be addressed by updating the structure into a two-wheel system which also boosts its performance. When transitioning from a

<sup>1</sup>Faculty of Electrical and Electronics Engineering, Universiti Malaysia, Pahang, Malaysia

<sup>2</sup>Faculty of Engineering, Universiti Malaysia, Pahang, Malaysia

<sup>3</sup>School of Engineering, London South Bank University, London, UK

## Corresponding author:

Nurul F Jamin, Universiti Malaysia, Pahang Kampus, Pekan 26600, Malaysia.

Email: [nunfadz86@gmail.com](mailto:nunfadz86@gmail.com)



four-wheeled to a two-wheeled structure to maintain the user's upright position, the system typically needs a high initial torque to lift the front wheel securely. A four-wheeled to two-wheeled wheelchair transformation will provide vertical reach for the user with height adjustment. Furthermore, the footprint of the wheelchair while on two wheels will be small and hence allowing it to manoeuvre in confined spaces. However, as a two-wheeled wheelchair is almost identical to an unstable, highly dynamic and nonlinear double-link inverted pendulum, but the control of the wheelchair is still a challenging process.

Ahmad and Tokhi<sup>1</sup> introduced an approach to lift the front wheels of a wheelchair having four wheels utilizing the linear quadratic regular (LQR) to transform the four-wheeled system into a two-wheeled wheelchair while stabilizing the system at an upright position based upon mathematical derivations. Ghani et al.<sup>2</sup> employed proportional integral derivative (PID) control to maintain wheelchair stability during ascending stairs. The findings also showed adequate system stability during both up stairs and down stairs manoeuvres. The system has demonstrated its steady performance during operation in an upright position with a simulated 1000 N disturbance (in force) at the wheelchair back-side with the use of a fuzzy logic control type-1 (FLCT1) controller. The study considered the system as a single-link inverted pendulum. Ahmad and Tokhi<sup>3</sup> have shown facilitation of manoeuvres and steering motions with a two-wheeled wheelchair in confined spaces using modular FLCT1. To ensure the stability of the wheelchair during steering movements, equivalent balancers have been introduced along with the aforementioned modular FLCT1. The authors have further reported the application of an analogous concept in the execution of both backward and forward motions.<sup>4</sup> In addition, as presented in Ahmad et al.,<sup>5,6</sup> FLCT1 has been assessed on many types of negative and positive perturbations at regular 10-s time spacing. Various forces ranging from  $\pm 100$  N to  $\pm 300$  N were applied to the seat's backside at repeated intervals of less than 10 s. The results exhibited that FLCT1 was effective in handling uncertainties without interrupting the stability of the wheelchair. However, due to the unpredictable disturbance, a displacement of 2 m was reported, with increased seat tilt recorded following the negative force's impact, and this phenomenon increased the settling time.

Rahman et al.<sup>7,8</sup> have reported the stability control of a mobile robot with two wheels using the LQR controller in a simulation environment based on state space model of the system. They have achieved good performance in controlling the Link1 and Link2's stability in an upright position. Nevertheless, the drawbacks mentioned in this research are that the LQR method is inefficient in managing unexpected disturbances, whereas their studies have overlooked the presence of human weight. Goher and Tokhi<sup>9</sup> have used a PID controller with a genetic algorithm (GA) for controlling a two-wheeled mobile robot. The method has been shown to maintain the system stability and increase the intermediate body's angular position.<sup>9</sup> Almeshal et al.<sup>10</sup> have used a combination of PID and PD controller in controlling a configurable two-wheeled double-link machine in the presence of external disturbances. However, a fairly large overshoot was observed following the vehicle's movement, which could not ensure the user's comfort. Moreover, Mostafa et al.<sup>11,12</sup> have investigated the stability and direction control of a two-wheeled robotic wheelchair through a movable payload mechanism using sliding-mode control under various disturbances. However, the wheelchair utilized single-link mechanism, and the movable payload was only placed by the added pendulum rod under the wheelchair seat and did not represent the real movement of the human disturbed by external forces.

A considerable amount of studies have been carried out on the stability of a double-linked pendulum system on the cart. These include LQR to ensure the stability of the system,<sup>13</sup> comparison of LQR–POI approaches to find the optimum stability,<sup>14</sup> investigation of the swing-up handling strategy,<sup>15</sup> and analysis of the ideal Riccati neural network equation along with the LQR method.<sup>16–18</sup> Researchers have also utilized model-free approaches using nonlinear control with unknown dynamics based on adaptive dynamic programming,<sup>19</sup> stability analysis of logical dynamic,<sup>20</sup> and cyclic-switched systems<sup>21,22</sup> with promising results. However, the literature is short of use of IT2FLC for stability of a two-wheeled wheelchair with moving payload. Furthermore, in the last decade, most scholars have emphasized on optimization techniques for achieving the most effective controller parameters as opposed to trial-and-error approaches. These techniques require considerable time to obtain the best control parameters for the system. Thus, the IT2FLC framework is introduced in this article to maintain the controller stability in a wheelchair with a moving payload simulated in SW4D software. SDA is then employed to determine the best controller gains. The performance of the designed controller is checked with numerous disruptions to represent real external forces, including moving payloads, that are sources of uncertainty in the system behaviour.

The rest of the article is structured as follows: “The two-wheeled wheelchair system” section illustrates the system model and parameters. The IT2FLC architecture is described in “Interval type-2 fuzzy logic controller design” section. “Spiral dynamic algorithm” section presents details of the experimental setup, and “Experimental setup” section provides the results and discussions. Finally, “Results and discussion” section concludes the article.

## The two-wheeled wheelchair system

In this research, the four-dimensional design software, namely SimWise 4 D (SW4D), is used to design a double-link inverted pendulum replicating a two-wheeled wheelchair. The system thus designed acts as a replacement to the mathematical model of a two-wheeled wheelchair, as it requires a shorter time-frame in deriving an accurate representation of the system. SW4D further has the advantage of introducing fixed nonlinearity, mass, gravity and friction of a two-wheeled wheelchair within the software environment. Thus, the complexity of the system can be maintained by using SW4D, and it does not rely on simplified mathematical modelling. Furthermore, conventional mathematical modelling cannot fulfil human logic and is far from representing real-world models. In addition, SW4D allows users to build models with various types of motors and joints, to test the models with uncertainties and various types of disturbances and to observe the movement of the models. Moreover, SW4D can be integrated with Matlab Simulink, thus allowing controller design and evaluation. In this manner, the SW4D can replicate the real hardware implementation since the developed model is based on the real model with visualization of the movement.

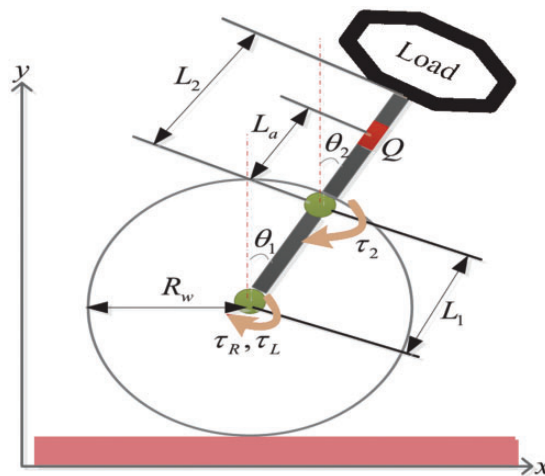
The two-wheeled wheelchair considered in this study accounts for a movable payload, whereby the seat can be moved up to a vertical range of 0.25 m, with the inclusion of a human load, using a linear actuation mechanism. Moreover, the design comprises a right wheel and a left wheel operated through independent motors on each wheel, and the system is modelled in the upright position. The Link1 is fixed on the centre of the bottom base, while Link2 is connected to the motors. The seat of the wheelchair is further connected to the linear actuator for height control, and the payload is attached above the seat in the form of a humanoid.

A schematic diagram of the two-wheeled wheelchair is presented in Figure 1, with the corresponding parameters shown in Table 1. As can be seen, link1 is locked at the centre of both right and left wheels, while link2 is connected to link1. The schematic diagram also shows the location of the radius of wheels, first link, second link, angular position for both links, linear actuator and the payload. All the wheels and links have their own masses, and the developed model has been implemented in SW4D where all the links and linear actuators can be controlled independently. The  $y$ -axis and  $x$ -axis are used for the angular and translational motions of the vehicle.

A complete model of the system design is further illustrated in Figure 2, with the inclusion of a concentrated force applied horizontally to the back of the seat, which represents the incoming simulated disturbances with a pulse signal during experimentation. Disturbances are applied in four specified conditions – (1) while the seat is moving upward, (2) while the seat is moving downward, (3) while the seat is extended to its maximum height and (4) while the seat is without any height extension. The physical dimensions of the system are presented in Table 2.

## Interval type-2 fuzzy logic controller design

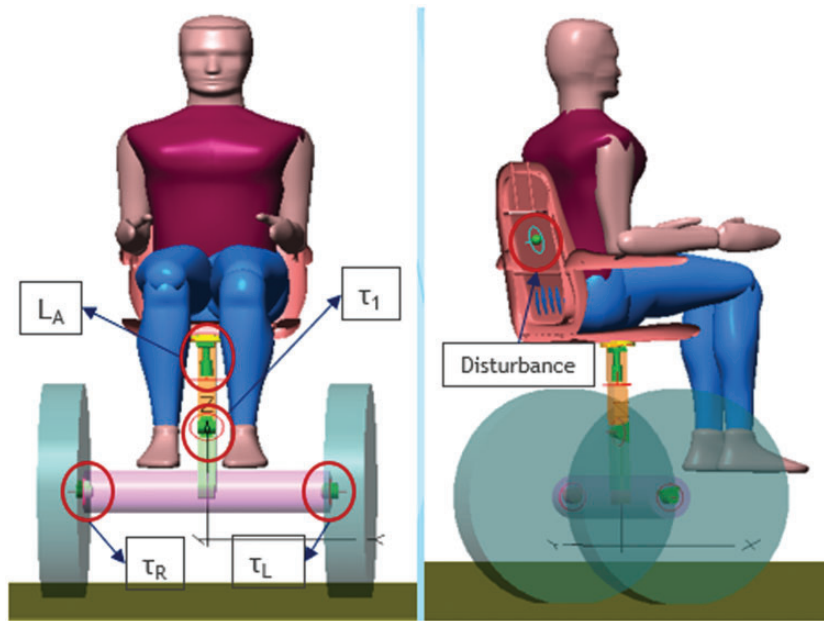
In 1975, Lotfi Zadeh implemented interval type-2 fuzzy logic for the first time. Over the past two decades, the term has become popular among researchers in the control context for complicated and challenging systems.<sup>23–29</sup> The technique is used for an extremely nonlinear method, namely stabilization of a two-wheeled, rotating



**Figure 1.** Schematic diagram of two-wheeled wheelchair.

**Table 1.** Components of two-wheeled wheelchair.

Symbol	Description	Unit
$\theta_1$	The angular position of Link1	$^\circ$
$\theta_2$	The angular position of Link2	$^\circ$
$R_w$	Radius of wheel	0.3 m
$\tau_R, \tau_L, \tau_2$	Torque at right/left wheel and between Link1 & Link2	Nm
$L_1$	Length of Link1	0.2 m
$L_2$	Length of Link2	0.22 m
$Q$	Displacement of the linear actuator	m
$L_a$	Length of the linear actuator from the upper link	m

**Figure 2.** Model of two-wheeled wheelchair in SimWise 4D.**Table 2.** Parameters for two-wheeled wheelchair.

Part	Size (m)	Weight (kg)
Wheel	Radius = 0.3, width = 0.09	1.500
Axle	Radius = 0.06, length = 0.55	20.00
Link1	Width = 0.04, length = 0.04, height = 0.2	3.000
Link2	Width = 0.04, length = 0.04, height = 0.22	3.000
Chair seat	Width = 0.4, length = 0.5, height = 0.101	0.205
Back rest	Width = 0.04, length = 0.04, height = 0.22	0.300
Humanoid	Height = 1.75 m	70.00

wheelchair with payload. The solution also takes into account the stability of Link1 and Link2 angular displacements in an upright position.

As shown in Figure 3, the IT2FLC comprises five key components: fuzzifier, rule base, inference engine, type reducer and defuzzifier. It should be remembered that the IT2FLC rules are identical to those of the FLCT1 with the type-2 fuzzy set (T2F set) input as well as output, as described in the Fuzzy Logic System rules. In combination with the inference engine, the fired rules map the T2FS input from the T2FS output.

It begins with the fused input variables (error and error change) into the T2FS data. The concept of IT2FLC is used in this context. Due to its suitability and usability for embedded processors and real-time applications, typically, a singleton fuzzification is used in this case. The inference engine and rule base activation,

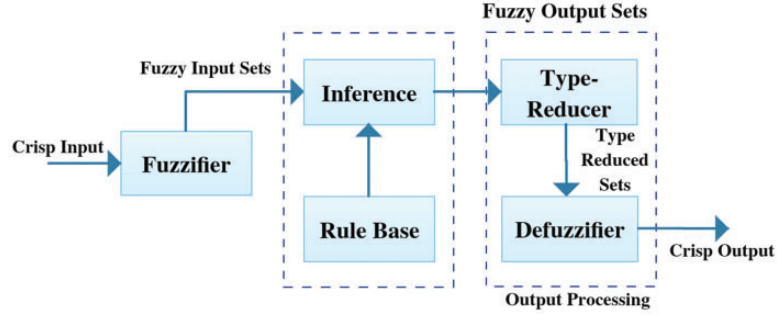


**Figure 3.** The architecture of interval type-2 fuzzy logic control.

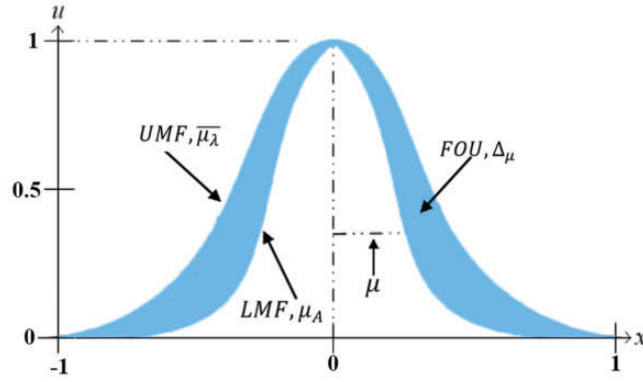


**Figure 4.** Interval type-2 fuzzy set.

which generate the output T2FS, are then triggered. The type reducer then processes this type-2 fuzzy output, explicitly using the Nie–Tan method for this analysis. The crisp value is obtained after the type reduction cycle is finished and the approximate type-reduced sets defuzzified and sent to actuators. A T2FS  $\tilde{A}$  is represented as follows

$$\tilde{A} = \int_{x \in X} \int_{u \in J_x} \mu_{\tilde{A}}(x, u) / (x, u), \text{ where } J_x \in [0, 1]$$

$$\tilde{A} = \int_{x \in X} \left[ \int_{u \in J_x} 1/u \right] / x, \text{ where } J_x \in [0, 1] \quad (1)$$

The FOU of  $\tilde{A}$  is represented as

$$FOU(\tilde{A}) = \bigcup_{x \in X} J_x = \{(x, u) : u \in J_x \subseteq [0, 1]\} \quad (2)$$

The FOU of  $\tilde{A}$  is comprised of two membership functions (MFs) (upper membership function (UMF) and the lower membership function (LMF) of  $\tilde{A}$ ) of type 1 which are shown in Figure 4. For FOU ( $\tilde{A}$ ), its upper bound (UMF) is presented as  $\bar{\mu}_{\tilde{A}}(x), \forall x \in X$ , while its lower bound (LMF) is given as  $\mu_{\tilde{A}}(x), \forall x \in X$ .<sup>30</sup> The UMF is given as

$$\bar{\mu}_{\tilde{A}}(x) = FOU(\tilde{A}) \quad \forall x \in X \quad (3)$$

Whereas the LMF is represented as

$$\mu_{\tilde{A}}(x) = FOU(\tilde{A}) \quad \forall x \in X \quad (4)$$

**Table 3.** Rules of interval type-2 fuzzy logic control.

$e/\Delta e$	NB	NS	Z	PS	PB
NB	PB	PB	PB	PS	Z
NS	PB	PB	PS	Z	NS
Z	PB	PS	Z	NS	NB
PS	PS	Z	NS	NB	NB
PB	Z	NS	NB	NB	NB

Various type-reduction methods can be used for T2FS including the Karnik–Mendel method<sup>31</sup> and the Karnik–Mendel enhanced method,<sup>32</sup> the uncertainty bound Wu–Mendel method,<sup>33</sup> the Nie–Tan method,<sup>30</sup> Bagain–Melek–Mendel method,<sup>32</sup> the Iterative Algorithm with Stop Condition<sup>34,35</sup> and the enhanced Iterative Algorithm with Stop Condition.<sup>36</sup>

As already suggested, in the current study, the Nie–Tan approach is used, as both type-reduction and defuzzification can be carried out simultaneously during the IT2FLC phase.<sup>37</sup> The Nie–Tan method is described as

$$y_{\text{crisp}} = \frac{\sum_{n=1}^N b_k \left( \bar{\mu}_{\tilde{A}^i}(x) + \bar{\mu}_{\tilde{A}^i}(x) \right)}{\sum_{n=1}^N \left( \bar{\mu}_{\tilde{A}^i}(x) + \bar{\mu}_{\tilde{A}^i}(x) \right)} \quad (5)$$

where  $b_k$  represents the centers of the output MFs, and  $\bar{\mu}_{\tilde{A}^i}(x)$  and  $\bar{\mu}_{\tilde{A}^i}(x)$  are the upper and lower membership grades of  $\tilde{A}^i(x)$ , respectively.

A total of five MFs of error, rate of error and output are defined; namely, Negative Big (NB), Negative Small (NS), Zero (Z), Positive Small (PS) and Positive Big (PB).

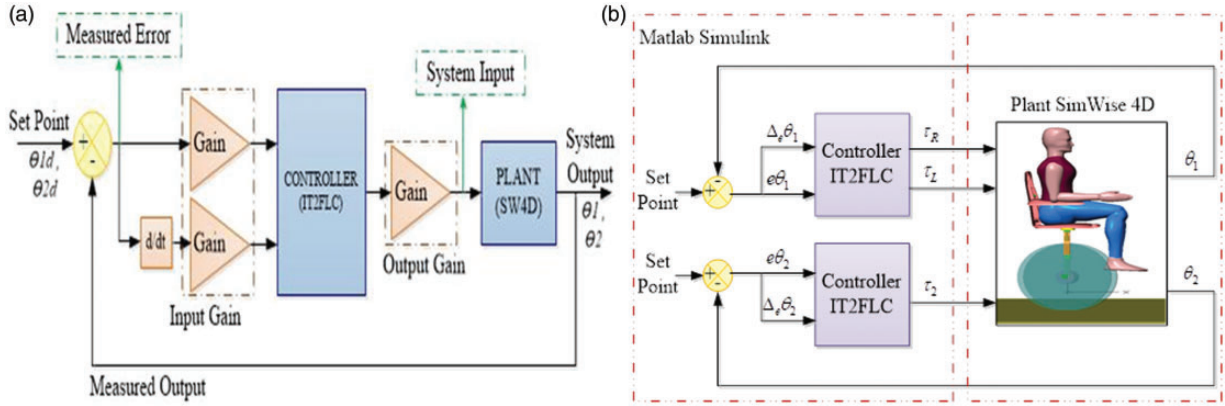
Different types of MFs in T2FS are recorded in the literature. These include trapezoidal, Gaussian and triangle-shaped types. Here, the Gaussian shape is utilized for all the inputs and outputs as it is easier to design and is simpler to represent and optimize. In addition, the Gaussian-shaped MFs takes shorter time to compute with shorter rule base, yet, provides comparatively good and smooth output results and steady responses of the two-wheeled wheelchair system than the other shapes. Figure 4 shows the T2FS with a boundary. The five Gaussian MFs for each input and output utilized in this paper possess the parameters of uncertain mean,  $\Delta\mu$ , and standard deviation,  $\sigma$  that needs to be optimized to acquire the system's optimal values. With the positions of the input MFs fixed between  $-1$  and  $+1$ , the standard values of  $\Delta\mu$  and  $\sigma$  have been noted at  $0.125$  and  $0.418$ , respectively.

The Mamdani inference is considered as a good option to use in this study, as it is easily understood, and its rules can be formulated, mainly with limitations in available information for the system.<sup>38</sup> Thus, Table 3 represents the MFs with five levels of each input and output, with 25 rules comprising the errors for angular positions, ( $e_i$ ) and the changes of error for angular position, ( $\Delta e_j$ ) of Link1 and Link2. The IF–THEN rule is further applied to produce the system's rule base, as follows

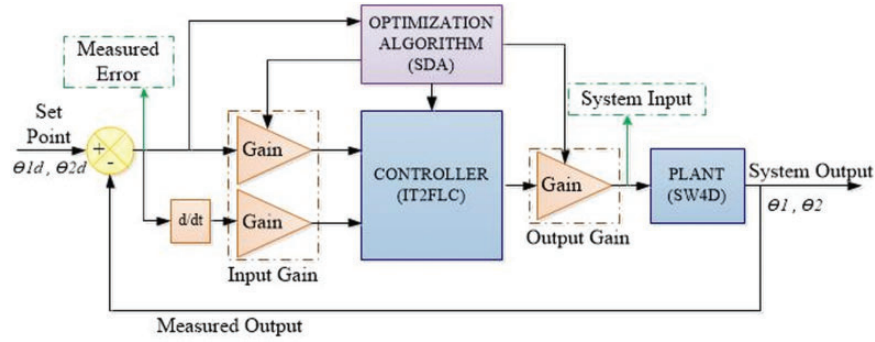
If  $e_i$  is NB and  $\Delta e_j$  is NB, then  $u$  is PB  
 If  $e_i$  is NB and  $\Delta e_j$  is NS, then  $u$  is PB  
 If  $e_i$  is NB and  $\Delta e_j$  is Z, then  $u$  is PB  
 If  $e_i$  is NB and  $\Delta e_j$  is PS, then  $u$  is PS  
 If  $e_i$  is NB and  $\Delta e_j$  is PB, then  $u$  is Z

Figure 5(a) shows the system's Simulink block diagram, where gains of the input/output are used to tune the fuzzy controller. The control input and output gains are employed to regulate both the input distribution of MFs and the distribution of output MFs. There are two control loops, namely IT2FLC1 and IT2FLC2, which have been designed to make the system stable, each with four input gains and two output gains. In total, 14 components must be optimized through SDA; eight input gain parameters and four output gain parameters,  $\Delta\mu$ , and  $\sigma$ . Figure 5(b) further illustrates the integration of the SW4D plant and the Matlab Simulink program.





**Figure 5.** (a) Simulink block diagram for the system; (b) integrated model for the system.



**Figure 6.** Block diagram of the optimization algorithm.

## Spiral dynamic algorithm

In order to improve the performance of the two-wheeled wheelchair system with movable payload, the SDA<sup>39</sup> is applied to obtain optimum values for the 14 parameters as noted in the previous subsection – input control gains, output control gains and controller gains for  $\Delta\mu$  and  $\sigma$  of IT2FLC.

Figure 6 shows the locations of the input control gains, output control gains and the controller gains in which the optimum parameters would be determined, with  $\Delta\mu$  as the blurred area of uncertainties in IT2FLC and  $\sigma$  as the width of the Gaussian MFs. Two control loops with four input control and two output control parameters need to be created in order to control the system stability.

Essentially, SDA is a two-dimensional metaheuristic algorithm proposed by Tamura and Yasuda in 2010. In 2011, it was derived into a general model for  $n$ -dimensional problems by the same authors. SDA is an uncomplicated search concept inspired by the spiral phenomenon that occurs within mother nature such as a nautilus shell, the galaxy, a tornado and a hurricane. Spiral models of the SDA are presented in Figure 7, where spiral models with  $\theta = \pi/4$ ,  $\theta = \pi/2$  and  $\theta = 2.4$  are illustrated in the left, middle and right models, respectively. It is realized that in SDA, all search agents or search points are designed to move towards the centre of the spiral from their outside area. Indirectly, this causes a constant decrease in the larger spiral step size, continuously converging towards its centre point.<sup>38</sup> The detailed operation of SDA is depicted in Table 4.

SDA is represented by two crucial parameters that affect the algorithm performance, in terms of the speed and accuracy of convergence, and these are the spiral radius ( $r$ ) and the rotation angle or displacement ( $\theta$ ).<sup>39</sup> The dynamic mathematical formula for the spiral radius of SDA is defined as

$$x_i(k+1) = S_n(r, \theta)x_i(k) - [S_n(r, \theta) - I_n]x^* \quad (6)$$

$$S_n = rR^n \quad (7)$$

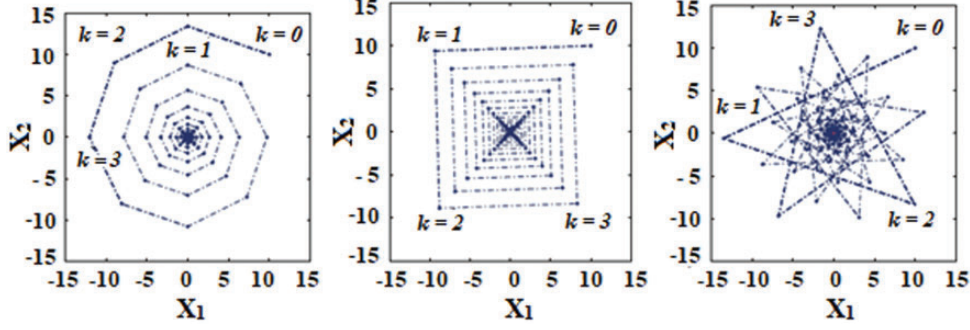


Figure 7. Spiral model for SDA.<sup>40</sup>

Table 4. Step of the SDA operation.

**Step 0: Preparation**

Select the number of search points  $m \geq 2$ , the parameter of  $0 \leq \theta < 2\pi$  and  $0 < r < 1$  of  $S_n(r, \theta)$  and the maximum number of iterations  $k_{\max}$ . Set  $k = 0$ .

**Step 1: Initialization**

Set initial points  $x_i(k+1) = S_n(r, \theta)x_i(k) - [S_n(r, \theta) - I_n]x^*$  in the feasible region and center as  $x^* = x_{i_g}(0)$ ,  $i_g = \arg\min_i f(x_i(0))$ ,  $i = 1, 2, 3, \dots, m$ .

**Step 2: Updating  $x_i$**

$x_i(k+1) = S_n(r, \theta)x_i(k) - [S_n(r, \theta) - I_n]x^*$   $i = 1, 2, 3, \dots, m$ .

**Step 3: Updating  $x^*$**

$x^* = x_{i_g}(k+1)$

$i_g = \arg\min_i f(x_i(k+1))$ ,  $i = 1, 2, 3, \dots, m$ .

**Step 4: Checking the termination criterion**

If  $k = k_{\max}$  then, terminate. Otherwise, set  $k = k + 1$  and return to step 2.

where  $i = 1, 2, 3, \dots, m$ ,  $I_n$  represents an identity matrix, and further variables are shown in Table 5.  $S_n$  is the multiplication of the radius,  $r$  and rotation matrix,  $R^n$ . An  $n$ -dimensional SDA is used in this paper due to the 14 parameters that need to be optimized to obtain the best optimal parameters. The rotation matrix for an  $n$ -dimensional SDA is defined as

$$R^n_{i,j}(\theta_{i,j}) = \begin{bmatrix} 1 & & & & & & & & & & & & & & & \\ & \ddots & & & & & & & & & & & & & & \\ & & 1 & & & & & & & & & & & & & \\ & & & \cos\theta_{i,j} & \cdots & & -\sin\theta_{i,j} & & & & & & & & \\ & & & & 1 & & & & & & & & & & \\ & & & \vdots & & \ddots & & \vdots & & & & & & & \\ & & & & & & 1 & & & & & & & & \\ & & & \sin\theta_{i,j} & \cdots & & \cos\theta_{i,j} & & & & & & & & \\ & & & & & & & 1 & & & & & & & \\ & & & & & & & & \ddots & & & & & & \\ & & & & & & & & & 1 & & & & & \end{bmatrix} \quad (8)$$

In this paper, the parameters of SDA,  $r = 0.95$  and  $\theta = \pi/4$  are used as the shape of spiral dynamic trajectory, with 50 search agents and 50 iterations. The mean square error (MSE) has been chosen as an objective function in this paper and defined as

$$MSE = \sqrt{\frac{1}{N} \sum_{i=1}^N (e^2)} \quad (9)$$



**Table 5.** Parameters of dynamic mathematical of SDA.

Parameter	Description
$\Theta$	Rotation angle or displacement
$r$	Spiral radius or convergence rate of distance between a point and the origin $0 \leq r \leq 1$
$x^*$	Centre point of a spiral
$S_n$	Multiplication of radius
$x_i$	Position of point
$k$	Number of iterations
$m$	Dimension of the search space
$i$	Number of points

**Table 6.** Boundaries of SDA.

Gains	Lower boundaries	Upper boundaries
K1	0.6500	1.650
K2	−0.475	0.525
K3	95.000	105.0
K4	3.6500	4.650
K5	−0.350	0.650
K6	45.000	55.00
K7	1.0500	2.050
K8	−0.255	0.545
K9	−205.0	−195.0
K10	6.6500	7.650
K11	−0.465	0.535
K12	−105.0	−95.0
K13	0.0500	0.200
K14	0.3600	0.460

where  $i = 1, 2, \dots, N$ ,  $e$  is the error in the angular position.

The goal of SDA is to eliminate errors in the angular positions of Link1 and Link2, as both the angles of Link1 and Link2 are stabilized in order to ensure that the two-wheeled wheelchair is positioned upright. The single objective function is therefore denoted as

$$F = w_1 MSE_1 + w_2 MSE_2 \quad (10)$$

where  $MSE_1$  is the error in the angular position of Link1,  $MSE_2$  is the error in the angular position of Link2,  $w_1$  is the weighted sum for error<sub>1</sub> and  $w_2$  represents the weighted sum for error<sub>2</sub>. The weight vector of this system is  $[w_1 \ w_2] = [0.7 \ 0.3]$ . Note that  $w_1$  is weighted larger than  $w_2$  because the angular position of Link1 in this system is more crucial to stabilize as compared to the angular position of Link2.

## Experimental setup

Simulation experiments are conducted in this section with the use of IT2FLC–SDA, in which the parameters for input and output control gains,  $\Delta\mu$ , and  $\sigma$  of the system are optimized through the SDA. In particular, three key experiments are conducted to investigate the robustness of the IT2FLC–SDA for the developed model. The first experiment looks into the undisturbed system performance for the static condition of the wheelchair, the second experiments tests the effect of various disturbances, the third experiment tests the effect of  $\pm 1000$  N disturbance with a height extension, the fourth experiment studies the system moving forward on a linear surface with  $\pm 1000$  N disturbance and the sixth experiment studies the system moving backward on a linear surface with  $\pm 1000$  N disturbance.

**Table 7.** Parameters of SDA.

Initialization parameter	Values
Number of dimensions	14
Spiral radius	0.95
Rotation angle	$\pi/4$
Number of particles	50
Number of iterations	50
A weighted sum of error1	0.7
A weighted sum of error2	0.3

**Table 8.** Extension of seat and external disturbance.

Experiment	Time (s)	Condition of seat	Force (N)
First experiment	0	Null	0
Second experiment	05.0	Normal	+100
	15.0	Maximum level	-100
	25.0	Maximum level	+150
	35.0	Normal	-150
	45.0	Normal	+200
	55.0	Maximum level	-200
	65.0	Maximum level	+250
	75.0	Normal	-250
	85.0	Normal	+300
	95.0	Maximum level	-300
	105	Normal	+350
Third experiment	10.0	Maximum height	-1000
	20.0	Normal	-1000
	25.5	Moving up	+1000
	35.5	Moving down	+1000
Fourth experiment	10.0	Maximum level	-1000
	20.0	Normal	-1000
	25.5	Moving up	+1000
	35.5	Moving down	+1000
Fifth experiment	15.0	Maximum level	-1000
	35.0	Normal	-1000
	60.5	Moving down	+1000
	80.5	Moving up	+1000

Tables 6 and 7 show the boundaries and parameters of SDA, respectively. Table 8 further shows the time intervals in which external disturbances are applied, the seat extension (height extension) of the two-wheeled wheelchair and the magnitudes of external disturbance applied to the back of the seat. The first experiment does not account for any extension in the height of the seat. External disturbances are applied for every 10 s, with the seat remaining at its normal condition, while the magnitude of the applied disturbance is increased from  $\pm 100$  to  $\pm 350$  N in the second experiment, and in the third experiment, disturbance magnitudes of  $\pm 1000$  N are applied at time intervals of 10, 15 and 20 s.

Furthermore, simple illustration on the forward and backward motion of the two-wheeled wheelchair system developed for this study between two independent locations (Point A and Point B) on a flat surface can be seen in Figures 8 and 9, respectively. The vertical extraction and retraction motions of the seat's height for the developed system are presented in Figure 10. As noted, the transformation in the seat's height extends to its maximum 0.25 m, while being able to retract back to its initial height. Figure 11 illustrates the directions of disturbances applied to the back of the seat during the experiments, whereby positive force is the disturbance applied in the forward direction and vice versa.

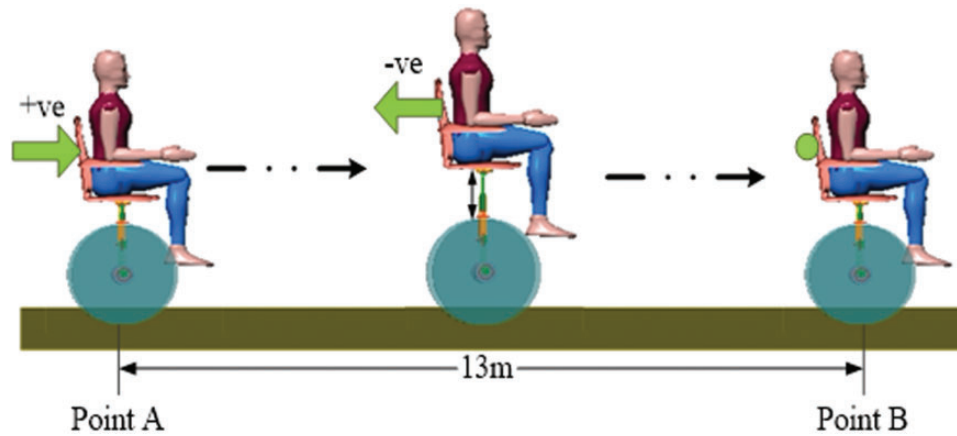


**Figure 8.** Two-wheeled wheelchair moving forward on the flat surface.

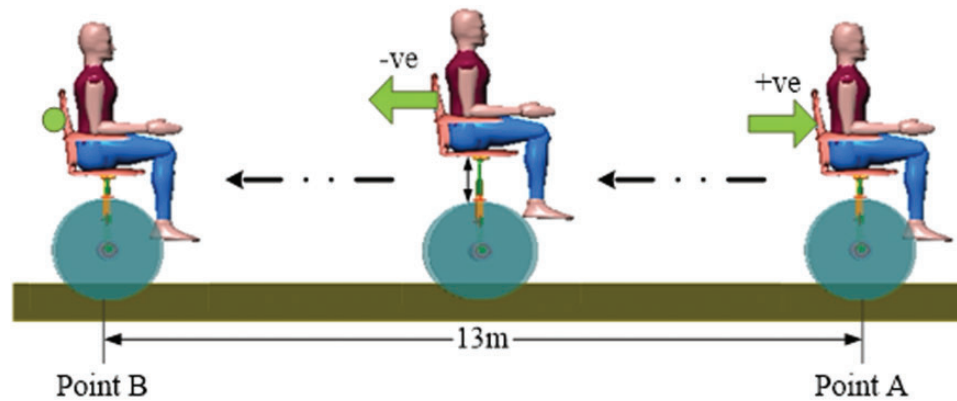


**Figure 9.** Two-wheeled wheelchair moving backward on the flat surface.

## Results and discussion

### Optimized parameters

As mentioned in the previous section, a total of 14 parameters have been accounted for optimization in this study in order to control the stability and motion of the two-wheeled wheelchair system with movable payload; eight parameters for input control gains, four parameters for output control gains and two parameters for controller gains. Following the optimized parameters developed through SDA, as detailed in Table 9, it is shown that the input control gains used were the lowest gain values, while the output control gains used were the highest gain values. As noted in Figure 12, the best fitness function of SDA steadily converged to 0.0052465 from iteration 23 until iteration 50.

### Undisturbed system performance

The first experiment was conducted on the developed two-wheeled wheelchair system under static condition, without disturbance exerted on system (undisturbed system) – external force would not be applied to the system, while linear actuator would not be activated to create the condition of movable payload. The performance comparison is accounted for between IT2FLC, alongside the proposed SDA–IT2FLC controller within the developed two-wheeled wheelchair system, and this can be further observed in Figure 13 in terms of travelled distance, torques on both wheels, torque between Link1 and Link2 and angular positions of both links.

The travelled distance for both approaches was close to 0 m since external force had not been applied to the system. However, fluctuations in the travelled distance are more significant at the initial phase of the simulation

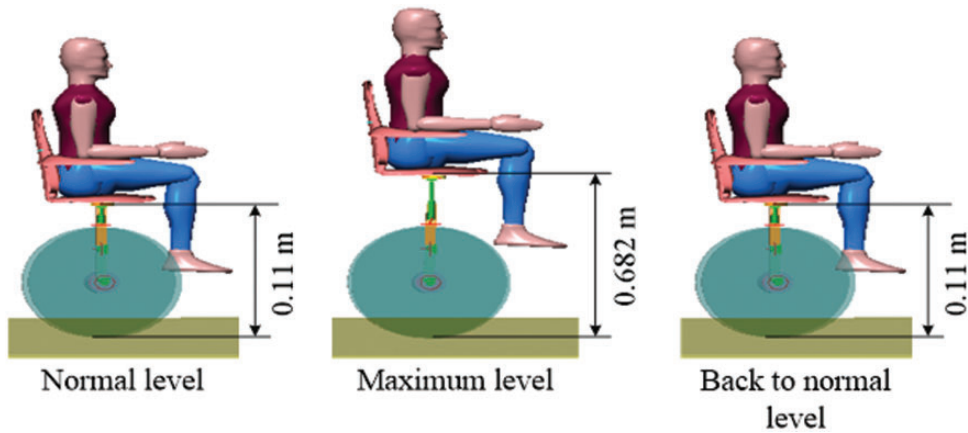


**Figure 10.** Height extension transformation of two-wheeled wheelchair.

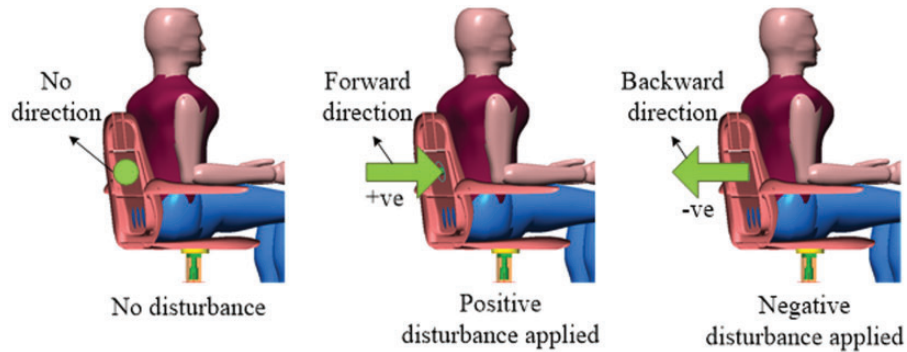


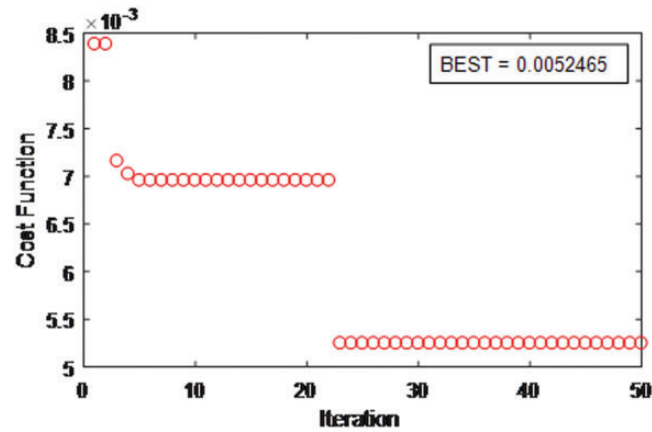
**Figure 11.** The direction of the positive and negative disturbance.

**Table 9.** Parameters of gain using SDA.

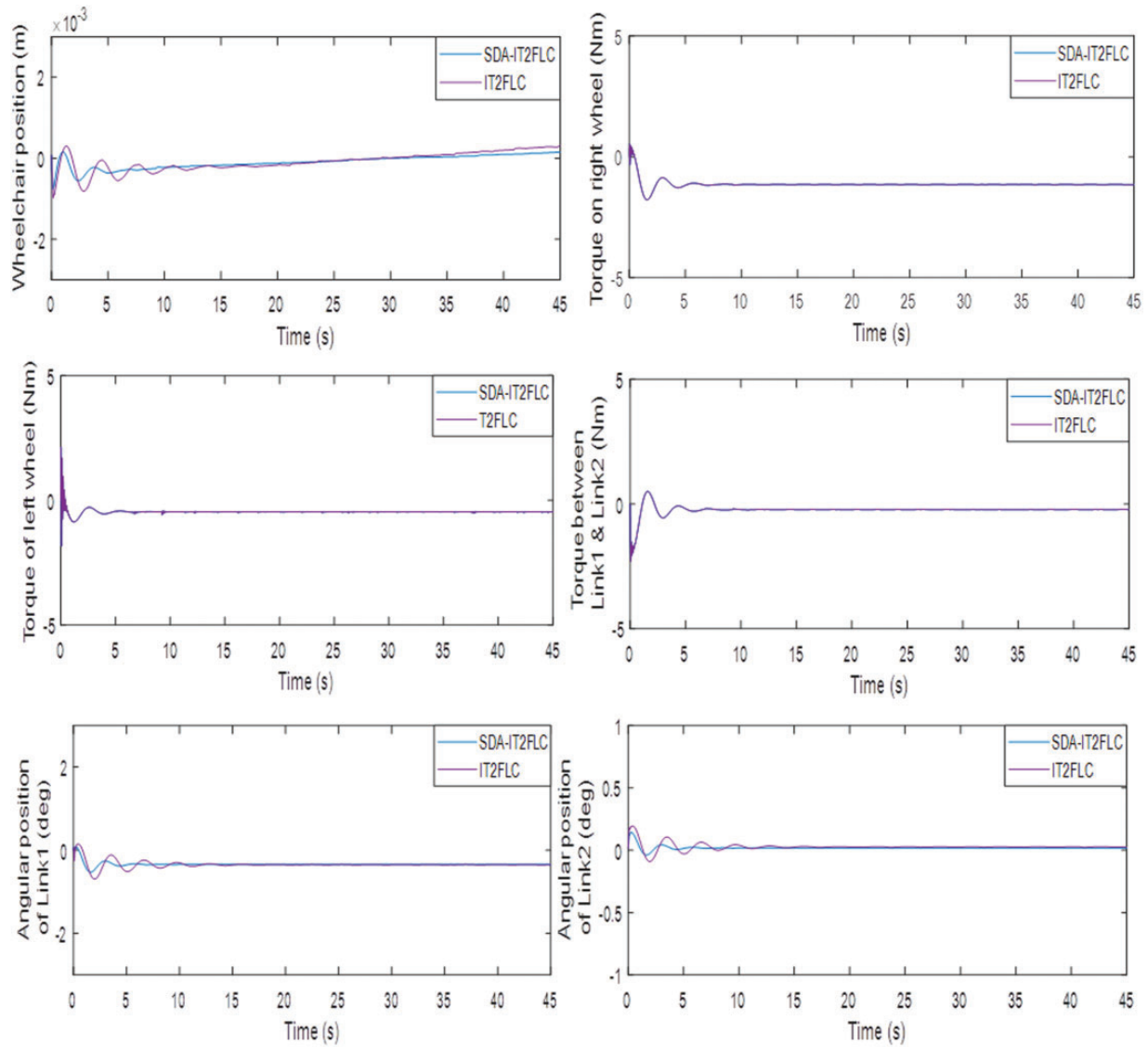
Gain	Parameters	SDA
K1	Input control gain	1.2199
K2	Input control gain	0.1321
K3	Output control gain	98.942
K4	Input control gain	3.6500
K5	Input control gain	0.1997
K6	Output control gain	45.106
K7	Input control gain	1.4854
K8	Input control gain	-0.455
K9	Output control gain	-205.0
K10	Input control gain	7.1834
K11	Input control gain	0.3109
K12	Output control gain	-105.0
K13	Delta	0.0500
K14	Sigma	0.3600

when IT2FLC was implemented, as against the implementation of SDA-IT2FLC. Moreover, torques for both wheels between Link1 and Link2 were recorded at  $<3$  Nm.

The system's angular positions as controlled through SDA-IT2FLC had outperformed IT2FLC in view of smaller angular positions for both links, with both yielding approximately  $0.3^\circ$  for Link1 and  $<0.05^\circ$  for Link2.



**Figure 12.** The best fitness function of SDA.

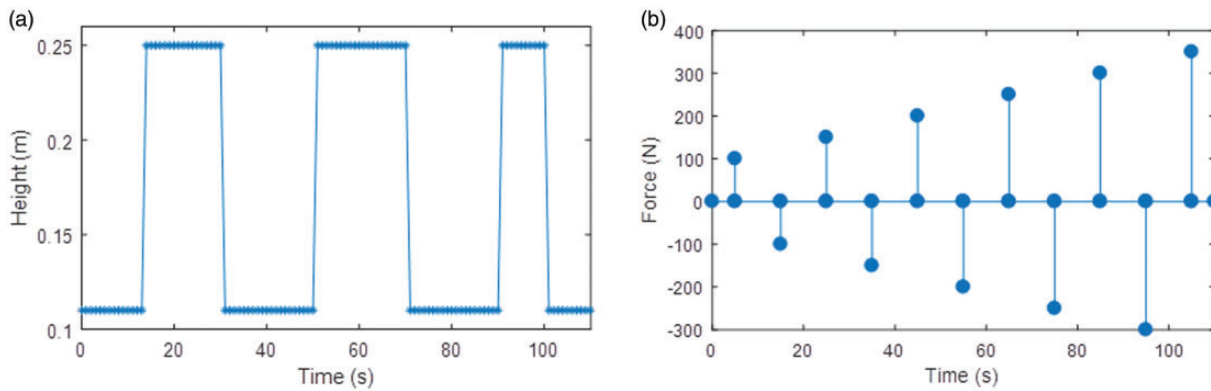


**Figure 13.** System performance of distance travelled, torques, Link1 and Link2 for undisturbed system.



**Table 10.** Performance comparison to the previous design for undisturbed system control of a static condition.

Aspect/paper	Current Performance	Ahmad et al. <sup>35</sup>
System	Two-wheeled wheelchair with a movable payload	Four-wheeled to a two-wheeled wheelchair
Controller	SDA-IT2FLC	FLCT1-GA
Settling time (s)	Between 5 and 7	All is 3
Angular position of Link1 (°)	<0.35	<1
Angular position of Link2 (°)	<0.03	<0.5
Peak Link1 (°)	0.1, -0.5	2, -5
Peak Link2 (°)	0.1, -0.04	2, -25
Peak torque right wheel (Nm)	±1.8	±45
Peak torque left the wheel (Nm)	±2.2	±45
Peak torque between L1L2 (Nm)	±2.3	±50

**Figure 14.** (a) Extension of seat; (b) various disturbance.

Attention is then brought to the settling time for SDA-IT2FLC at 5 s, which has been comparatively shorter than that recorded for IT2FLC, which, yet again, outshined performance of the heuristic approach.

The proposed SDA-IT2FLC was placed into comparison with the previously designed FLCT1 with GA optimization (FLCT1-GA) system.<sup>35</sup> Upon recorded information on both controllers in Table 10, the proposed controller, which has surpassed that of heuristic IT2FLC under similar conditions, has prevailed as a better approach, in view of angular positions for both links as well as peak angle amplitudes of Link1 and Link2. Furthermore, a 93% reduction in the system's torque has been achieved, which represents significant improvement within the system's control and performance.

### Effect of various disturbances

A comparison was made to verify the robustness of IT2FLC-SDA against the controller in a previously reported design,<sup>5,6</sup> where the same pattern of disturbances was applied to the system. Previous studies have focused on examining the robustness of FLCT1 in controlling the stability of a two-wheeled wheelchair, under varying positive and negative disturbances at magnitudes of up to  $\pm 350$  N. The stability of the two-wheeled wheelchair in the previous design has been controlled using FLCT1. Herewith, the system within the current study was simulated under similar circumstances, with the application of optimized parameters.

The system was disturbed with increasing disturbances at  $\pm 100$  N,  $\pm 300$  N and  $+350$  N at 10-s intervals, with an upward and downward moving payload to up to 0.25 m, as shown in Figure 14(a). Forward and backward motions were also applied accordingly following the application of positive and negative forces based on their directions as shown in Figure 14(b).

As noted, the two-wheeled wheelchair system could withstand positive and negative disturbances up to a force of 350 N with a settling time of less than 10 s for all disturbances, as can be seen in Figure 15. At a high negative disturbance of  $-300$  N, the distance by which the system was displaced (travelled distance) and recorded at an

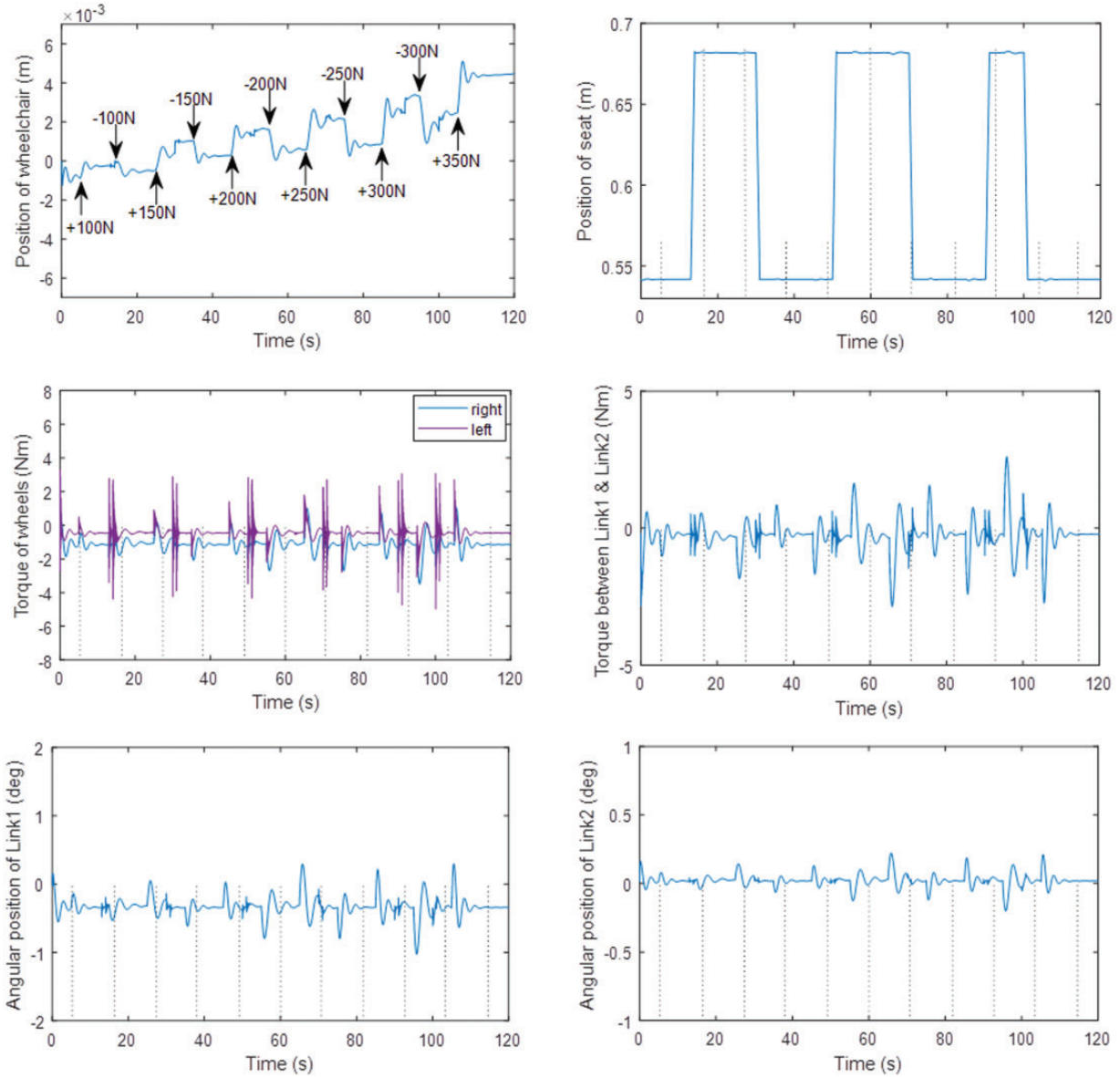


**Figure 15.** System performance of distance travelled, height extension of seat, torques, Link1 and Link2 with various disturbances.

approximate value of 0.002 m; whereas, at the highest positive disturbance of 350 N, the travelled distance was recorded at a value of less than 0.03 m.

It is worth mentioning that the torques after perturbed with external disturbances for both Link1 and Link2 were larger in previous works<sup>5,6</sup> with  $\pm 50$  N, as compared to the controller tested in this work, with a mere torque of  $\pm 3$  N on both links; there was a reduction of 94%. Moreover, the travelled distances of the system due to various positive and negative forces were much shorter than the previous design, with a reduction of up to 98.5%. The previous design had yet to include the movable payload mechanism and had been simpler in comparison to the current system. The proposed IT2FLC–SDA controller has proven its ability to handle a more complex and highly nonlinear system, specifically for a two-wheeled wheelchair with the inclusion of a movable payload.

#### *Effect of $\pm 1000$ N disturbance with height extension*

For the second experiment, the two-wheeled wheelchair system with movable payload was tested with both application of external disturbances and height transformation of the seat while the system remained static in

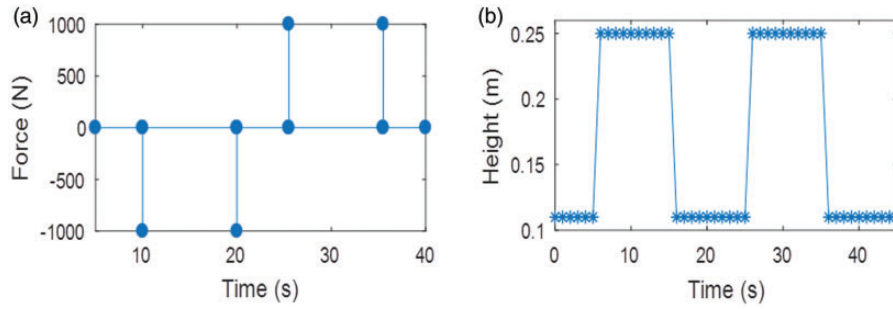


**Figure 16.** External disturbance and the position of seat for second experiment.

a location. FLCT1 was not compared with the proposed IT2FLC–SDA in this context as findings from the first experiment have proven the superiority of the proposed controller to that of the previous design.

Therefore, unlike the previous experiment, the robustness of IT2FLC–SDA for the developed two-wheeled wheelchair system was hereby tested through the application of greater external disturbances of up to  $\pm 1000$  N on the back of the seat, while the seat was extended to a maximum height of approximately 0.25 m. Four main conditions were accounted in which the external disturbances were applied:

- at 10 s when the payload was extended to the maximum height.
- at 20 s when the payload was maintained without any extension (normal condition).
- at 25.5 s while the payload was moving upward to reach a higher level of the seat.
- at 35.5 s while the payload was moving downward after having reached a higher level.

In summary, graphs showing external disturbances and the positions of the seat following the proposed time intervals are shown in Figure 16. The system's performance, including the displacement of the two-wheeled wheelchair and its seat, the torques of Link1 and Link2, as well as the angular positions of Link1 and Link2, are presented in Figure 17. As noted, the displacement for the designed system was recorded at less than 0.05 m when SDA was applied. Thus, it is evident that a force with high magnitude to the wheelchair possesses an insignificant effect on its stability. Note that this simulation was conducted to examine the robustness of IT2FLC–SDA embedded within the two-wheeled wheelchair in controlling its stability in an upright position, with considerable uncertainties and nonlinearities. Thus, the ability of the proposed controller has been shown in tackling well the safety issue encountered by wheelchair users when faced with great disturbances from unexpected external sources.

Moreover, a more significant result, in terms of maximum overshoot and undershoot, is proven to be more achievable through applying the parameters of SDA to the two-wheeled wheelchair system with a movable payload. Among other overshoots due to disturbances, the utmost crucial observation ultimately lies in the maximum overshoot of the torque for Link1 and Link2 following the disturbance of +1000 N, specifically at 25.5 s when the payload moved upward to reach its maximum height, and at 35.5 s when the payload moved downward back to its original state.

Optimized parameters through SDA have also improved the system's performance in terms of traveling time and distance. Among all the disturbances applied, the settling time required for the wheelchair has been within 10 s, even after perturbed with forces as large as  $-1000$  N at the 20 s and  $+1000$  N at 25.5 s. Based on these improvements, it is clear that the IT2FLC–SDA can handle nonlinearities and uncertainties in ensuring the stability of a two-wheeled wheelchair, with a movable payload.

### *Moving forward on linear surface with $\pm 1000$ N*

The third experiment hereby tests the robustness of IT2FLC–SDA control of the two-wheeled wheelchair, in managing incoming external disturbances of  $\pm 1000$  N, particularly during forward motion on a flat surface, while accounting for height adjustments of the payload. With mirroring the second experiment in this work, the current experiment would not present a comparison to the previous design; yet, it includes a forward motion as an additional aspect for consideration.

Figure 18 shows the forms of external disturbances exerted on the system and the positions of the seat over the stated time intervals, with the inclusion of a forward motion specified to a distance of 8 m. Herewith, the

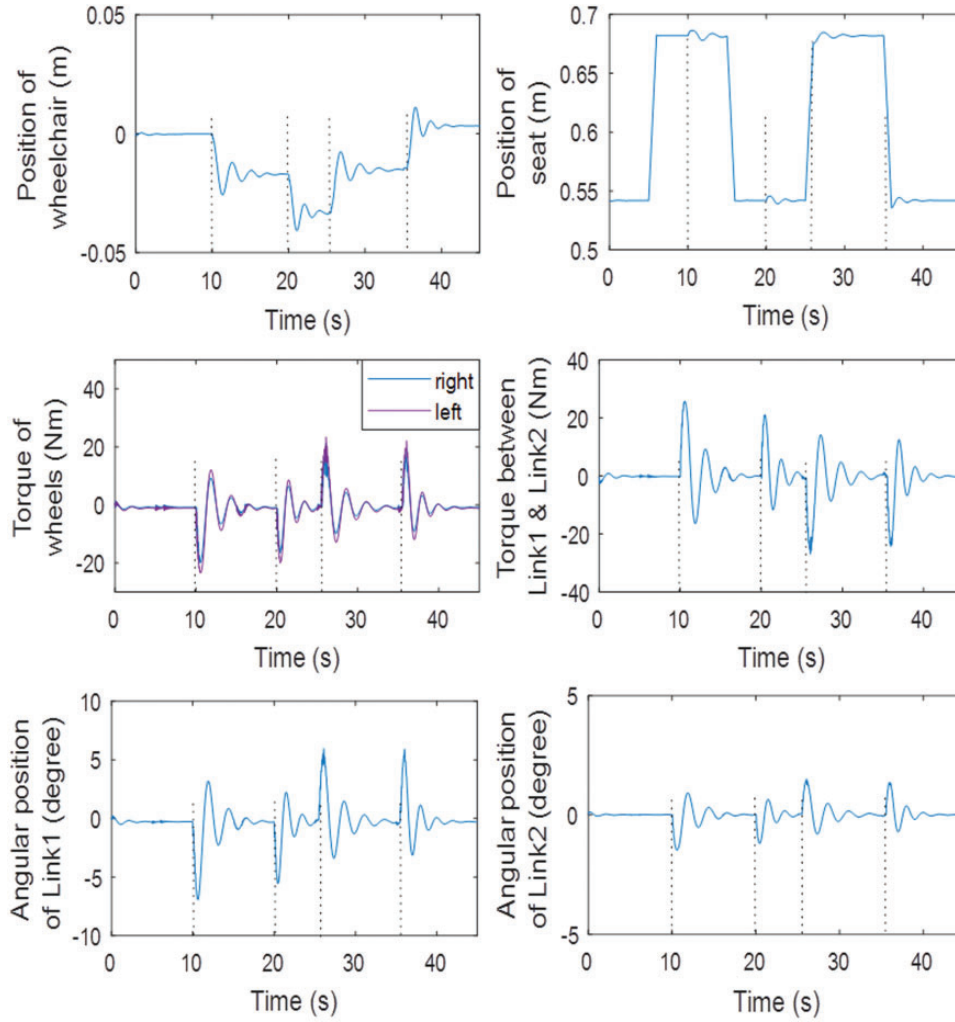


**Figure 17.** System performance of displacement, torques, Link1 and Link2 with  $\pm 1000$  N.

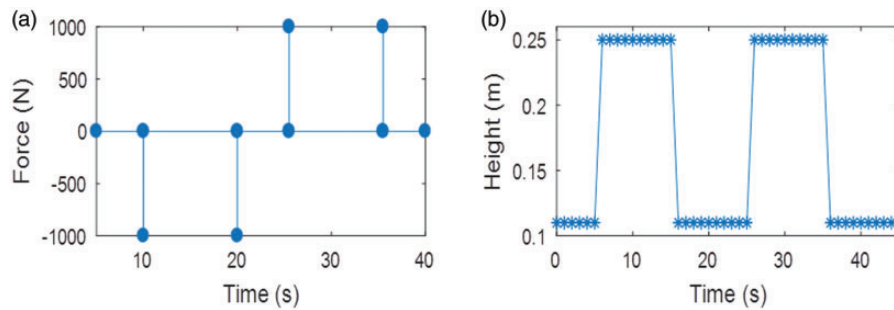


**Figure 18.** (a) External disturbance and (b) the position of seat for third experiment.

robustness of IT2LC is examined for the time-frames similar to those of the second experiment, under the situation where the two-wheeled wheelchair system is moving forward, and its payload is vertically extended and retracted simultaneously.

The results of system's performance are presented in Figure 19, with observations placed on the displacement of the two-wheeled wheelchair, torques of Link1 and Link2 and angular positions of Link1 and Link2 when the system is disturbed with a force of  $\pm 1000$  N under the situations outlined in Table 7; similar to those of the second experiment.

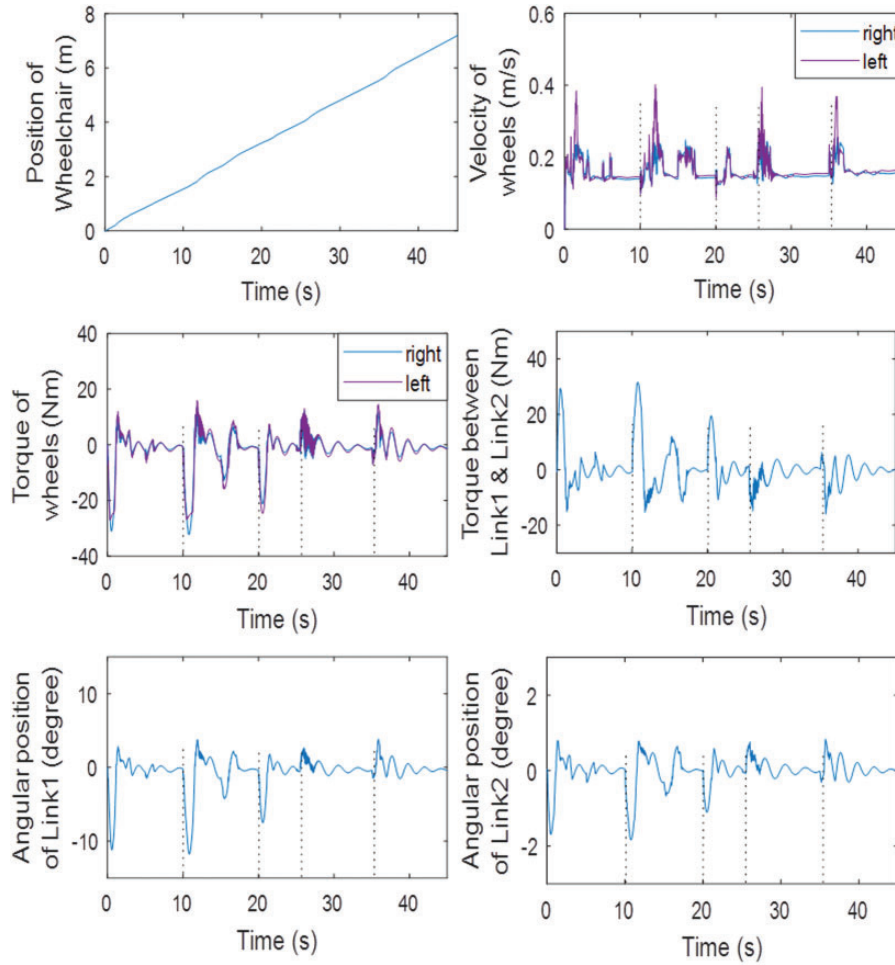


**Figure 19.** System performance of two-wheeled wheelchair while moving forward on a flat surface with  $\pm 1000$  N.

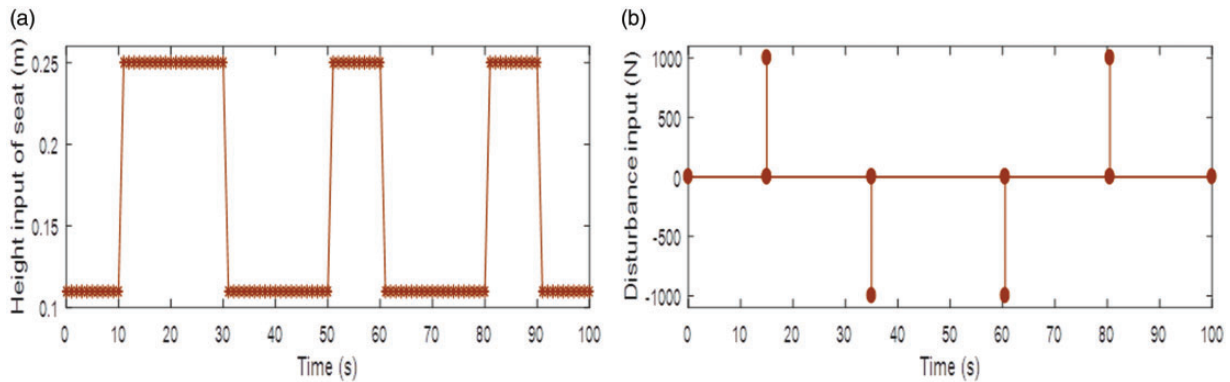


**Figure 20.** (a) External disturbance and (b) the position of seat for third experiment.

With the system moving forward up to 8 m with the height adjustment of the movable payload, the results show that both Link1 and Link2 merely required a small amount of torque of less than  $\pm 30$  Nm when the velocity of the system was at about 0.3 m/s. It is found that larger angular positions of both links were recorded following the disturbance of  $-1000$  N at 10 and 20 s, confirming that negative disturbances have a more significant impact on the system's stability and demonstrates that as compared to positive disturbances, the system is more challenging to control.



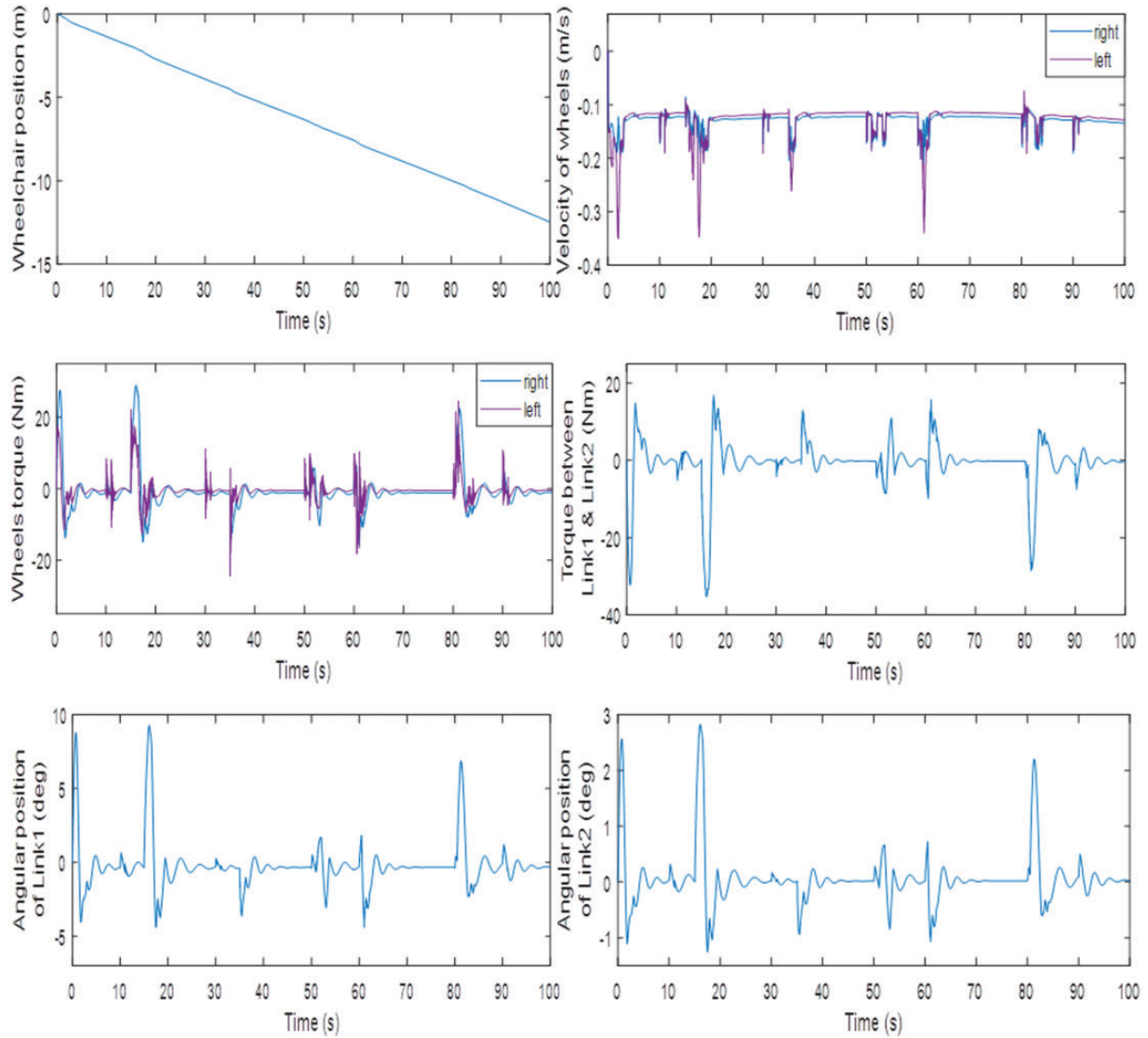


**Figure 21.** System performance of two-wheeled wheelchair while moving backward on a flat surface with  $\pm 1000$  N.

Priority has been placed on crucial conditions of the system, especially when the payload is moving upward and downward; yet, the system has proven its ability to withstand disturbance forces of up to  $\pm 1000$  N under such conditions when moving forward on a flat surface. Despite minor oscillations recorded in this experiment, the proposed controller has confirmed its effectiveness to stabilize the system in an upright position after perturbed by external disturbances while carrying a payload of approximately 70 kg.

#### *Moving backward on linear surface with $\pm 1000$ N*

The last experiment was conducted to control the system in backward motion with disturbance. The robustness of the proposed controller (IT2FLC–SDA) was tested with the combination of positive and negative disturbance forces of  $\pm 1000$  N in the form of pulses applied to the back of the seat. Figure 20(a) shows the height input of the seat at which the disturbance was applied to the system to allow the payload on seat moving in upward and downward direction.

The system was simulated to travel in 100 s, and the seat was moved up to the maximum height of 0.25 m. Figure 20(b) shows the disturbance  $\pm 1000$  N applied in four main conditions:

- at 15 s when the payload was moved to the maximum height.

- at 35 s when the payload was maintained without any movement (normal condition).
- at 60.5 s while the payload was moving downward after having reached the maximum height.
- at 80.5 s while the payload was moving upward to reach a higher level.

Figure 21 shows the system's performance thus achieved. The system travelled up to 13 m over the given time with a velocity of  $-0.15$  m/s in a stable manner with movable payload and disturbance rejection even though there was small fluctuation at 15 and 60.5 s. This shows that the system was influenced by the combination of positive and negative forces that made the payload to tilt forward and backward accordingly.

The torques of the system consist of those at both right and left wheels and between Link1 and Link2. As can be noted, there were significant differences in terms of angle and torque for both links when applied with positive and negative forces.

The positive force (forward direction) caused the torque on the system to increase up to  $+30$  Nm at 15 and 80.5 s, while the negative force (backward direction) only resulted in a low torque of  $-15$  Nm. This also happened in case of the torque between Link1 and Link2, where the torque was quite high after the application of positive forces at 15 and 80.5 s with approximately  $-35$  Nm, while the torque was less than  $+20$  Nm after application of negative forces at 35 and 60.5 s.

Based on the results shown, the angular position was higher with positive disturbance force at 15 and 80.5 s in comparison to the application of the negative disturbance force. The result of angular displacement for Link1 was  $10^\circ$  and  $7^\circ$  after disruption with  $+1000$  N (15 and 80.5 s) and about  $4^\circ$  after disruption with  $-1000$  N at 35 and 60.5 s. The result of angular displacement for Link2 was less than  $3^\circ$  after the application of positive and negative forces; it only reached  $-1^\circ$  after disturbed at 35 and 60.5 s. Based on the system performance, it is shown that the proposed IT2FLC–SDA can control backward motion on a flat surface with movable payload and disturbance rejection in 100 s.

## Conclusion

This study has presented the IT2FLC–SDA method to stabilize a two-wheeled wheelchair with a movable payload, while the wheelchair has been designed and simulated in the SW4D software. The robustness of the designed controller has been examined in this study. The performance of the system has also been investigated in a simulated environment using Matlab Simulink and SW4D software.

Through experiments conducted, it has been shown that the IT2FLC–SDA has outperformed FLCT1–GA (used in a previous design) in terms of angular position for both Link1 and Link2 as well as peak torques of the system with 93% reduction in torque. In addition, the robustness of the controller has been examined with application of external disturbances of  $\pm 1000$  N in four situations including the seat moved to its peak position, the seat in its original position, the seat moving upwards to its highest point and the seat moving back to its original position. The efficiency of the system using the IT2FLC–SDA has also been observed to be excellent with respect to the over-and-under-shoot when simulated with optimum parameters via the SDA. This has been exhibited by torques reported from Link1 to Link2 to below  $\pm 30$  Nm during application of external disturbances.

The designed controller, IT2FLC–SDA, has been found to develop low torques both for Link1 and Link2 after application of positive and negative disturbances between  $\pm 100$  and  $\pm 300$  N. With similar disturbances of earlier studies, around 94% decrease of torque between Link1 and Link2 and a decrease of more than 98% of travel distance due to external disturbances in comparison with the earlier scheme have been observed. Although previous studies emphasize the fixed-load method, the present study has taken into account the dynamic case of moving payloads. The study thus has shown that the IT2FLC–SDA controller is excellent in handling a system with uncertainties and nonlinearities, such as the two-wheeled wheelchair, even in the presence of external disturbances of up to  $\pm 1000$  N, overall seating height adjustments at around 0.25 m and a moving payload as well as when the system is moving backward and forward.

The current research has considered a two-wheeled wheelchair system confined to plain surfaces in simulation experiments, with the application of external disturbances and height transformation. A wheelchair system that moves up and down a sloped surface will serve as a separate area for further research to improve the wheelchair system design while improving performance and safety. Moreover, the real hardware implementation will be considered a further area of research as future work.

## Declaration of conflicting interests

The author(s) declared no potential conflicts of interest with respect to the research, authorship, and/or publication of this article.

## Funding

The author(s) disclosed receipt of the following financial support for the research, authorship, and/or publication of this article: The work is supported by the Faculty of Electrical and Electronics Engineering, Universiti Malaysia Pahang, with the assistance of Grant PGRS170344 and the Ministry of Higher Education of Malaysia, under the Mybrain15 scheme.

## ORCID iD

Nurul F Jamin  <https://orcid.org/0000-0002-5182-4566>

## References

1. Ahmad S and Tokhi MO. Linear quadratic regulator (LQR) approach for lifting and stabilizing of two-wheeled wheel-chair. In: *4th international conference on mechatronics*, Kuala Lumpur, Malaysia, 17–19 May 2011.
2. Ghani NMA, Tokhi MO, Nasir ANK, et al. Control of a stair climbing wheelchair. *Int J Robot Automat* 2012; 1: 203–213.
3. Ahmad S and Tokhi MO. Steering motion control enhancement scheme of two wheeled wheelchair in confined spaces. *Int J Automat Control Eng* 2013; 2: 179–189.
4. Ahmad S and Tokhi MO. Forward and backward motion control of wheelchair on two wheels. In: *3rd IEEE conference on industrial electronics and applications* 2008, pp.461–466.
5. Ahmad S, Siddique NH and Tokhi MO. A modular fuzzy control approach for two-wheeled wheelchair. *J Intell Robot Syst* 2011; 64: 401–426.
6. Ahmad S, Siddique NH and Tokhi MO. Modelling and simulation of double-link scenario in a two-wheeled wheelchair. *J Integr Comp-Aided Eng* 2014; 21: 119–132.
7. Rahman MTA, Ahmad S, Akmeliawati R, et al., Centre of gravity (C.O.G)-based analysis on the dynamics of the extendable double-link two-wheeled mobile robot. In: *5th international conference on mechatronics*, Kuala Lumpur, Malaysia, 2–4 July 2013.
8. Rahman MTA, Ahmad S and Akmeliawati R. Integrated modeling and analysis of an extendable double-link two-wheeled mobile robot. In: *IEEE/ASME international conference on advanced intelligent mechatronics* 2013, pp.1798–1803.
9. Goher KMK and Tokhi MO. and Genetic algorithm based modeling and control of a two wheeled vehicle with an extended rod, a Lagrangian based dynamic approach. In: *IEEE 9th international conference on cybernetic intelligent systems*, Berks, UK, September 2010.
10. Almeshal AM, Goher KM and Tokhi MO. Dynamic modelling and stabilization of a new configuration of two-wheeled machines. *Robot Autonom Syst* 2013; 61: 443–472.
11. Mostafa N, Loulin H and Ahmed MA. Stability and direction control of a two-wheeled robotic wheelchair through a movable mechanism. *IEEE Access* 2020; 8: 45221–45230.
12. Mostafa N, Loulin H and Ahmed MA. An approach on velocity and stability control of a two-wheeled robotic wheelchair. *Appl Sci* 2020; 10: 1–18.
13. Yadav SK, Sharma S and Singh N. Optimal control of double inverted pendulum using LQR controller. *Int J Adv Res Comp Sci Softw Eng* 2012; 2: 189–192.
14. Singh N and Yadav SK. Comparison of LQR and PD controller for stabilizing double inverted pendulum system. *Int J Eng Res Dev* 2012; 1: 69–74.
15. Henmi T, Deng M and Inoue A. Swing-up control of a serial double inverted pendulum. In: *Proceedings of the 2004 American control conference*, 2004, pp.3992–3997.
16. Wei H, Qian Q, Qiang H, et al. Optimization of sliding mode controller for double inverted pendulum based on Genetic Algorithm. In: *2nd international symposium on systems and control in aerospace and astronautics*, 2008.
17. Lashin M and Ramadan A. Optimal design of a state feedback sliding mode controller of a loaded double inverted pendulum (Preprint Submitted to Elsevier). *IEEE Control Syst Mag*, October 2015.
18. Lashin M, Ramadan A, Abbass HS, et al. Design of an optimized sliding mode control for loaded double inverted pendulum with mismatched uncertainties. In: *19th international conference on methods and models in automation and robotics*, 2014, pp.270–275.
19. Sun T and Sun X-M. An adaptive programming scheme for nonlinear optimal control with unknown dynamics and its application to turbofan engines. In: *IEEE transactions on industrial informatics*, 2020, pp.1–9. Piscataway, NJ: IEEE.
20. Sun T, Wang R, Zhao X, et al. Partial and global stabilization at an attractor for k-valued logical control networks. *J Frank Inst* 2020; 357: 7003–7019.
21. Sun T, Sun X-M, Gao Y, et al. Stability analysis of logical networks with switching signal and control input. *Nonlinear Anal Hybrid Syst* 2020; 36: 1–18.

22. Sun T, Liu T and Sun X-M. Stability analysis of cyclic switched linear systems: an average cycle dwell time approach. *Inform Sci* 2020; 544: 227–237.
23. Bardini ME and Nagar AME. Interval type-2 fuzzy pid controller for uncertain nonlinear inverted pendulum system. *J ISA Trans* 2014; 53: 732–743.
24. Hsiao MY and Wang CT. A finite-time convergent interval type-2 fuzzy sliding-mode controller design for omnidirectional mobile robots. In: *International conference on advanced robotics and intelligent systems*, 2013, pp.80–85.
25. Hagrass HA. A hierarchical type-2 fuzzy logic control architecture for autonomous mobile robots. *IEEE Trans Fuzzy Syst* 2004; 12: 524–539.
26. Farooq U, Gu J and Luo J. An interval type-2 fuzzy lqr positioning controller for wheeled mobile robot. In: *IEEE international conference on robotics and biomimetics*, 2013, pp.2403–2407.
27. Ri MH and Huang J. Design of interval type-2 fuzzy logic controller for mobile wheeled inverted pendulum. In: *12th world congress on intelligent control and automation*, 2016, pp.535–540.
28. Nagar AME, Bardini ME and Rabaie NME. Intelligent control for nonlinear inverted pendulum based on interval type-2 fuzzy PD controller. *Alexandria Eng J* 2014; 53: 23–32.
29. Hsiao MY, Chen CY and Li THS. Interval type-2 adaptive fuzzy sliding-mode dynamic control design for wheeled mobile robots. *Int J Fuzzy Syst* 2008; 10: 268–275.
30. Nie M and Tan WW. Towards an efficient type-reduction method for interval type-2 fuzzy logic systems. In: *IEEE international conference on fuzzy systems (IEEE world congress on computational intelligence)*, 2008, pp.1425–1432.
31. Mendel JM. Super-exponential convergence of the Karnik–Mendel algorithms for computing the centroid of an interval type-2 fuzzy set. *IEEE Trans Fuzzy Syst* 2007; 15: 309–320.
32. Wu D, Mendel JM. Enhanced Karnik–Mendel algorithms. *IEEE Trans Fuzzy Syst* 2009; 17: 923–934.
33. Wu H and Mendel JM. Uncertainty bounds and their use in the design of interval type-2 fuzzy logic systems. *IEEE Trans Fuzzy Syst* 2002; 10: 622–639.
34. Duran K, Bernal H and Melgarejo M. Improved iterative algorithm for computing the generalized centroid of an interval type-2 fuzzy set. In: *Proceeding annual meeting of the North American fuzzy information processing society*, 2008, pp.1–5.
35. Ahmad S, Tokhi MO and Toha SF. Genetic algorithm optimisation for fuzzy control of wheelchair lifting and balancing. In: *EMS 2009 – UKSim 3rd European modelling symposium on computer modelling and simulation*, 2009, pp.97–101.
36. Wu D and Nie M. Comparison and practical implementation of type reduction algorithms for type-2 fuzzy sets and systems. In: *Proceeding IEEE international conference fuzzy systems*, 2011, pp.2131–2138.
37. Wu D. Approaches for reducing the computational cost of interval type-2 fuzzy logic systems: overview and comparisons. *IEEE Trans Fuzzy Syst* 2013; 21: 80–99.
38. Ghani NMA and Tokhi MO. Simulation and control of multipurpose wheelchair for disabled/elderly mobility. *Integr Comp-Aid Eng* 2016; 23: 331–347.
39. Ghani NMA, Nasir ANK and Tokhi MO. Optimization of fuzzy logic scaling parameters with spiral dynamic algorithm in controlling a stair climbing wheelchair: ascending task. In: *19th international conference on methods and models in automation and robotics*, 2014, pp.776–781.
40. Tamura K and Yasuda K. Primary study of spiral dynamics inspired optimization. *IEEJ Trans Elec Electron Eng* 2010; 6: 98–100.